Development 137, 2571-2578 (2010) doi:10.1242/dev.053801

Negative control of Smad activity by ectodermin/Tif1γ patterns the mammalian embryo

Leonardo Morsut[1,*], Kai-Ping Yan[2,*,†], Elena Enzo[1], Mariaceleste Aragona[1], Sandra M. Soligo[1], Olivia Wendling[3], Manuel Mark[2,3], Konstantin Khetchoumian[2], Giorgio Bressan[1], Pierre Chambon[2,3], Sirio Dupont[1], Régine Losson[2,‡] and Stefano Piccolo[1,§]

SUMMARY

The definition of embryonic potency and induction of specific cell fates are intimately linked to the tight control over TGFβ signaling. Although extracellular regulation of ligand availability has received considerable attention in recent years, surprisingly little is known about the intracellular factors that negatively control Smad activity in mammalian tissues. By means of genetic ablation, we show that the Smad4 inhibitor ectodermin (*Ecto*, also known as *Trim33* or *Tif1γ*) is required to limit Nodal responsiveness in vivo. New phenotypes, which are linked to excessive Nodal activity, emerge from such a modified landscape of Smad responsiveness in both embryonic and extra-embryonic territories. In extra-embryonic endoderm, *Ecto* is required to confine expression of Nodal antagonists to the anterior visceral endoderm. In trophoblast cells, *Ecto* precisely doses Nodal activity, balancing stem cell self-renewal and differentiation. Epiblast-specific *Ecto* deficiency shifts mesoderm fates towards node/organizer fates, revealing the requirement of Smad inhibition for the precise allocation of cells along the primitive streak. This study unveils that intracellular negative control of Smad function by ectodermin/Tif1γ is a crucial element in the cellular response to TGFβ signals in mammalian tissues.

KEY WORDS: Nodal, Smad ubiquitin ligase, Spemann Organizer and mesoderm patterning, TGFβ signaling, Early mouse embryo

INTRODUCTION

The TGFβ cascade is a fundamental player in mammalian development and adult tissue homeostasis. TGFβ signals through cognate serine/threonine receptors and leads, intracellularly, to the activation of the R-Smad/Smad4 transcriptional complex (Moustakas and Heldin, 2009). Although TGFβ ligands are widely expressed in tissues, they can elicit their effects in a strict temporally and spatially controlled manner. For the signal to reach only the appropriate cells and with the correct intensity, mechanisms must be in place to determine where and when cells must not respond to TGFβ. This layer of regulation is just as likely to play a key role in defining cell fate as the signal itself, as suggested by phenotypes emerging from inactivation of extracellular TGFβ antagonists (Bachiller et al., 2000; Perea-Gomez et al., 2002; Zacchigna et al., 2006).

In addition to regulation in the extracellular space, intracellular control mechanisms also exist. One example is the phosphorylation/dephosphorylation cycle of receptor-Smads (Itoh and ten Dijke, 2007; Lin et al., 2006). Recently, we have proposed a parallel layer of control of Smad activity centered on a cycle of monoubiquitylation and deubiquitylation of Smad4, which is mediated, respectively, by ectodermin (Ecto, also known as Tif1γ or Trim33) and FAM/Usp9x (Dupont et al., 2009). Through these inhibitory systems, Smad transcriptional complexes are disassembled and R-Smads are forced to exit the nucleus and check the activity status of the receptors. It has been proposed that this mechanism avoids saturation of the signaling cascade, maintaining Smad activity proportional to – and finely tunable by – variations in extracellular ligand concentrations (Moustakas and Heldin, 2009). Despite these speculations, it remains unclear to what extent these negative regulatory steps impact on TGFβ responsiveness in vivo. Here, we used the mouse embryo as a model system to tackle this issue.

During early vertebrate embryogenesis, the graded activity of the TGFβ-related factor Nodal orchestrates the maintenance or restriction of embryonic pluripotency and establishes the body plan. In the mouse, Nodal induces and patterns the anterior visceral endoderm (AVE), and sustains trophoblast development. These tissues then provide fundamental instructive signals to the epiblast, cooperating with Nodal itself to induce the mesoderm and endoderm germ layers and to pattern them along the anteroposterior axis during gastrulation (Arnold and Robertson, 2009; Tam and Loebel, 2007). In recent years, systematic inactivation of positive transducers of the Nodal pathway indicated that cells of the embryo are able to interpret very subtle variations in Nodal signaling, as indicated, for example, by the phenotype of *Nodal* hypomorphic alleles (Norris et al., 2002) or by the requirement of *Smad4* only for high-threshold responses (Chu et al., 2004). Yet, what generates such graded Nodal signaling activity in vivo is less clear. In this paper, we provide evidence that a negative intracellular Smad regulator, ectodermin, plays an essential role in how cells read TGFβ signals.

[1]Department of Medical Biotechnologies, Section of Histology and Embryology, University of Padua, viale Colombo 3, 35126 Padua, Italy. [2]Institut de Génétique et de Biologie Moléculaire et Cellulaire (IGBMC), Department of Functional Genomics, CNRS/INSERM/ULP/Collège de France. [3]Institut Clinique de la Souris (ICS), BP 10142, 67404 Illkirch-Cedex, France.

*These authors contributed equally to this work
‡Present address: The Wistar Institute, 3601 Spruce Street, Philadelphia, PA 19104, USA
‡Deceased; this paper is dedicated to Regine's memory
§Author for correspondence (piccolo@civ.bio.unipd.it)

Accepted 26 May 2010

MATERIALS AND METHODS

Generation of *Ecto* knockout and conditional alleles

To generate the *Ecto/Tif1g* targeting vector, a genomic clone spanning exons 2, 3 and 4 was used (Yan et al., 2004). Briefly, a *loxP* flanked (floxed) *PGK-Neo* cassette was inserted within the first intron, and a third *loxP* site was inserted within the fourth intron (see Fig. S1 in the supplementary material). The targeting fragment was electroporated into 129/Sv H1 ES cells as described previously (Cammas et al., 2000). After selection, neomycin-resistant ES clones were expanded, and their genomic DNA was screened by PCR. Positive clones were further validated with Southern blotting analysis with two independent probes (not shown). ES cells bearing the correctly targeted allele were injected into C57BL/6 blastocysts to produce chimeric offspring. These were backcrossed with C57BL/6 mice, and their offspring was genotyped by PCR. Mice heterozygous for the targeted allele were then crossed with *CMV-Cre* transgenic mice (Dupe et al., 1997), and the offspring was analyzed by PCR to identify animals with either complete recombination of the *loxP* sites (null allele, *Ecto–*) or lacking of the *PGK-Neo* cassette owing to recombination of the first and second *loxP* sites (conditional allele, *Ecto fl*). *Cre*-negative $Ecto^{+/-}$ and *Ecto fl/fl* mice were subsequently kept on a C57BL/6 background for phenotypic analyses. Animal care was in accordance with our institutional guidelines.

Generation of *Ecto-EpiKO* and compound $Ecto^{-/-}$; $Smad4^{-/-}$, $Ecto^{-/-}$; *Nodal*Δ*600/–* embryos

To obtain epiblast-specific *Ecto* knockout embryos, *Sox2-Cre;* $Ecto^{+/-}$ males were crossed with *Ecto fl/fl* females. In this setup, the *Sox2-Cre* transgene selectively deletes the floxed alleles in ICM/epiblast cells (Hayashi et al., 2002). Embryos were genotyped after in situ hybridization for *Ecto fl*, *Ecto*+, *Ecto–* and *Cre* alleles. Embryos were scored as mutants in the presence of *Cre*, *Ecto fl*, *Ecto–* and absence of *Ecto*+ alleles.

To obtain embryos homozygous null for both *Ecto* and *Smad4*, *Ecto fl/fl*; *Smad4 fl/fl* (Bardeesy et al., 2006) males were crossed with *CAG-Cre*; $Ecto^{+/-}$; $Smad4^{+/-}$ females. In this setup, the Cre protein supplied by the mother within the oocyte completely recombinates the paternal floxed alleles after fertilization, irrespective of transgene transmission (Sakai and Miyazaki, 1997), raising the expected frequency of compound null embryos to 25%. Embryos were genotyped after in situ hybridization for *Ecto fl* (recognizing also the *Ecto*+ allele), *Ecto–*, *Smad4 fl* (recognizing also the *Smad4*+ allele) and *Smad4–* alleles. Embryos were scored as compound mutants in the presence of *Ecto–* and *Smad4–*, and in the absence of *Ecto fl* and *Smad4 fl* alleles.

To obtain $Ecto^{-/-}$ embryos with reduced Nodal signaling, $Ecto^{+/-}$; $Nodal^{+/-}$ [*lacZ* allele (Collignon et al., 1996)] mice were crossed with $Ecto^{+/-}$; *Nodal+/*Δ*600* (Norris et al., 2002) mice. Embryos were genotyped after in situ hybridization for *Ecto*+, *Ecto–*, *lacZ* and *Nodal*Δ*600* alleles.

Phenotype characterization

Mouse embryos were staged based on their morphology, considering the morning of the vaginal plug as E0.5. Embryos were manually dissected in ice-cold DEPC-treated phosphate-buffered saline (PBS) and fixed overnight in PBS 4% PFA at 4°C, dehydrated (for storage) and rehydrated through methanol series. Whole-mount in situ hybridizations were performed according to http://www.hhmi.ucla.edu/derobertis/ (*Xenopus* ISH protocol), with minor modifications to ensure efficient genotyping after staining: day 1, post-fixing after proteinase K treatment was carried out with 4% PFA only, 1 hour at 4°C; day 3, washes were carried out with PBS 0.5% goat serum (GS, Invitrogen), without AP1 incubation before BM-Purple staining (Roche), and without post-fixation. Embryos were mounted in 80% glycerol and photographed with a Leica DMR microscope equipped with a Leica DC500 camera. Unless otherwise indicated, embryos of different genotypes stained with the same marker are shown at the same magnification. For each experiment, at least five embryos of every genotype were analyzed with consistent results.

For immunostaining, embryos were fixed overnight in PBS 4% PFA supplemented of phosphatase inhibitors (Sigma) at 4°C, dehydrated and rehydrated through methanol series. Embryos were permeabilized with two washes in PBS 0.5% NP40 for 20 minutes at 4°C, followed by one wash in PBS 0.3% Triton X-100 for 20 minutes at room temperature. After two washes in PBS 0.1% Triton X-100 (PBT) for 15 minutes at room temperature, embryos were blocked with two washes in PBT 10% GS for 1 hour at room temperature, and incubated overnight with rabbit anti-Ecto primary antibody (Sigma HPA004345, 1:75) in PBT 10% GS or in rabbit mAb anti-phospho-Smad2 (CST-3108, 1:50) in PBT 3% BSA. The following day, embryos were washed twice in PBT 2% GS for 15 minutes at 4°C, and five more times in PBT 2% GS for 1 hour at 4°C. Secondary Alexa555 goat anti-rabbit antibody (1:200) was incubated overnight in PBT 5% GS. The third day, embryos were washed five times in PBT for 15 minutes at room temperature, mounted in 80% glycerol and photographed with a Nikon Eclipse E600 confocal microscope equipped with a Bio-Rad Radiance2000 camera/laser scanning system. Nuclear localizations were confirmed by colocalization with YOYO1 staining (Invitrogen). Specificity of the phospho-Smad2 signal was confirmed by incubating E6.0 wild-type embryos for 8 hours in 10 μM SB431542 TGF-β receptor inhibitor, causing disappearance of the signal (not shown).

For histological analysis, deciduae were collected in PBS, fixed in Bouin's overnight, dehydrated and embedded in paraffin. Serial sections were cut at 6 μm and stained with Hematoxylin and Eosin according to standard procedures. Similar procedures were applied to obtain sections of embryos after in situ.

Genotyping

Offspring were genotyped by PCR on genomic tail DNA extracted by standard procedures. After in situ, individual embryos were manually dissected with a tungsten wire (FineScienceTools) to eliminate the EXE and ectoplacental cone, thus avoiding maternal DNA contaminations. Epiblast/VE tissues were lysed overnight at 55°C with mild agitation in 10 mM Tris/HCl (pH 8.0), 50 mM KCl, 2 mM $MgCl_2$, 0.3% Tween-20, 0.5% NP-40 supplemented with fresh proteinase K (Invitrogen, 1:40). Lysis volume was adjusted according to the stage: E5.5, 20 μl; E6.5, 40 μl. After vortexing, proteinase K was inactivated for 10 minutes at 95°C, quenched on ice, and samples were centrifuged for 10 minutes at 4°C at 10,000 ***g***. 4ul of the fresh supernatants were used for each PCR reaction using EX-Taq polymerase (Takara). For detection of the *Ecto–* allele in embryos of early stages, nested PCR was employed if necessary.

TS cell culture and RT-PCR analysis

TS cells were cultivated and passaged in feeder-free conditions as indicated previously (Oda et al., 2006). pLKO lentiviral shRNA targeting mouse Ecto was purchased from Sigma (5′-CCGGCGTGTGATAGAT-TGACGTGTACTCGAGTACACGTCAATCTATCACACGTTTTTG-3′). Control shGFP sequence was as described previously (Adorno et al., 2009). Lentivirally infected populations were established by puromycin selection as indicated previously (Moffat et al., 2006). For differentiation assays, TS cells were seeded and grown for 2 days in stem-cell medium; undifferentiated samples were allowed to differentiate further in the same conditions for 2 days; differentiated samples were changed to DMEM 10% FCS (t=0) and cultivated for the indicated times, renewing the culture medium every 2 days. TGFβ stimulation was provided by adding every day 100 ng/ml Activin-A (Peprotech) directly to the medium. Cultures were harvested in Trizol (Invitrogen) for RNA extraction, and contaminant DNA was removed by DNAse treatment. Real-time qPCR analyses were carried out on triplicate samplings of retrotranscribed cDNAs with RG3000 Corbett Research thermal cycler and analyzed with Rotor-Gene Analysis6.1 software. Experiments were performed at least twice, with duplicate biological replicates.

RESULTS

Ectodermin is required for early mouse embryonic patterning

To investigate the role of Ecto in vivo, we generated *Ecto* conditional and germline knockout alleles (see Fig. S1 in the supplementary material for details on the targeting procedure and validation of effective loss-of-Ecto). Mice heterozygous for the *Ecto*-null mutation ($Ecto^{+/-}$) were viable and fertile; however,

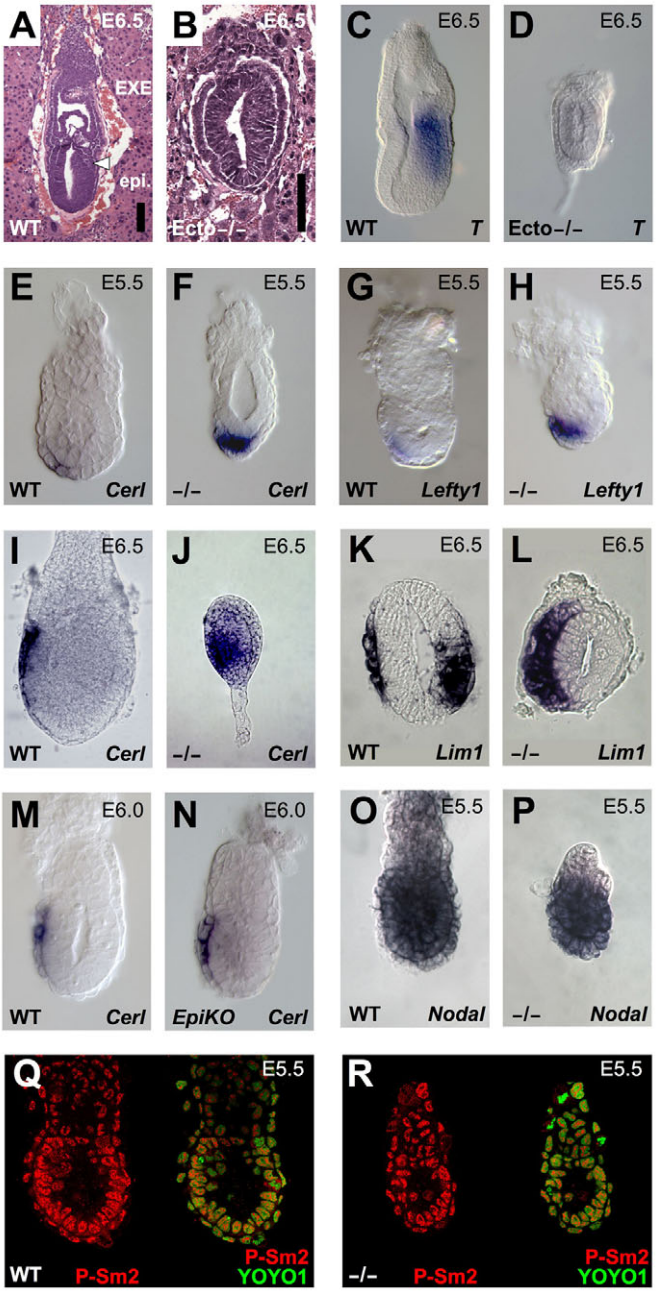

Fig. 1. *Ecto* homozygous mutant embryos display profound defects in polarity and patterning before gastrulation. (**A**,**B**) Hematoxylin and Eosin staining of sections of wild-type (A) and *Ecto*$^{-/-}$ (B) embryos within intact decidual tissues at early-streak stage. Primitive streak formation is absent (arrowhead) and the embryo lacks a distinction between epiblast (epi.) and extra-embryonic ectoderm (EXE). Scale bars: 10 μm. (**C**,**D**) E6.5 *Ecto* mutant embryos do not express the pan-mesodermal marker *T* (also known as *Brachyury*). See Fig. S2 in the supplementary material for other mesoderm markers. (**E-H**) At earlier stages, AVE is strongly expanded in *Ecto* mutants, as assayed by expression of the Nodal/Smad targets *Cerl* (E,F) and *Lefty1* (G,H). (**I-L**) As development proceeds, the AVE of *Ecto*-deficient embryos further expands, encircling the epiblast. (I,J) Lateral views, anterior towards the left, of early-streak stage embryos stained for *Cerl*. (K,L) Transverse paraffin sections of early-streak stage embryos stained for *Lim1*, anterior is towards the left. Although in wild-type embryos *Lim1* stains both the AVE and the primitive streak, in *Ecto* mutants the AVE is much broader and the mesodermal expression domain of *Lim1* is lost. For a whole-mount lateral view of *Lim1* expression on wild-type and *Ecto* mutants, see Fig. S2G,H in the supplementary material. (**M**,**N**) *Ecto* acts cell-autonomously within the extra-embryonic tissues to restrain AVE formation. Panels show in situ for *Cerl* at pre-streak stage in wild-type and *Sox2-Cre;Ecto fl/–* (*Ecto-EpiKO*) embryos, i.e. in embryos where *Ecto* is inactivated in epiblast cells, but not in extra-embryonic tissues. (**O**,**P**) *Nodal* is normally expressed in *Ecto* mutants at E5.5, but it is rapidly downregulated as development proceeds (see also Fig. S2 in the supplementary material). (**Q**,**R**) Smad2 is normally activated in *Ecto* mutants, as assayed by immunofluorescence for phospho-Smad2 (Yamamoto et al., 2009) (P-Sm2, red channel). Merged images with nuclear counterstain are also shown (YOYO1, green channel).

homozygosity resulted in embryonic lethality. Indeed, embryos from heterozygote intercrosses were collected at different stages of gestation and *Ecto* mutants could be recovered at the expected Mendelian ratios at E5.5 to E7.5, but not at later stages.

Morphological and histological analyses demonstrated that *Ecto* mutants display striking defects in embryonic polarity and tissue patterning. When compared with control littermates, E6.5 *Ecto* mutants were smaller and lacked a clear distinction between epiblast and extra-embryonic ectoderm (EXE). Wild-type embryos formed mesoderm as a consequence of gastrulation; by contrast, *Ecto* mutants could readily be identified by the undivided proamniotic cavity and the lack of a primitive streak (Fig. 1A,B). Defective mesoderm formation was confirmed by in situ hybridization at early streak stage examining the expression of markers, such as *T*, *Eomes* and *Wnt3* (Fig. 1C,D; see Fig. S2 in the supplementary material). For these analyses and throughout the study, we analyzed at least five embryos of each genotype with consistent results; figures show representative phenotypes.

At first, lack of mesoderm in *Ecto* mutants came as a surprise, as this phenotype was opposite to the excessive mesoderm differentiation displayed by Ecto-depleted *Xenopus* embryos (Dupont et al., 2005). However, in contrast to amphibians, mesoderm formation in the mammalian embryo is a late event, requiring inputs from the EXE and AVE extra-embryonic lineages. As the development of such tissues relies on the activity of early-acting Nodal/Smad4 signaling (Arnold and Robertson, 2009), we tested whether defects in *Ecto* mutants initiated with abnormal extra-embryonic development. Expression of AVE markers at E5.5 was strikingly upregulated in *Ecto* mutants: when these markers were barely detectable in wild-type littermates, signals of the Nodal targets *Cerberus-like* (*Cerl*; *Cer1* – Mouse Genome Informatics), *Lefty1* and *Lim1* (Lhx1 – Mouse Genome Informatics) mRNAs were already strong in knockout embryos, becoming rapidly saturated in an abnormally broad AVE domain (Fig. 1E-H and not shown). Although in E6.5 wild-type embryos AVE markers are usually restricted to an anterior narrow stripe of cells, in *Ecto* mutants, robust *Cerl* and *Lim1* expression was expanded around the epiblast (Fig. 1I-L; Fig. S2G,H in the supplementary material).

Ectodermin is expressed ubiquitously in early mouse embryos by immunofluorescence (see Fig. S1E,G in the supplementary material and data not shown). Genetic evidence indicates that AVE responds to Nodal ligands emanating from the epiblast (Lu and Robertson, 2004). Thus, we next tested the possibility that AVE expansion in Ecto mutants is caused by a cell-autonomous enhanced Smad responsiveness, as opposed to being secondary to increased ligand expression/availability in the epiblast. To achieve

this, we made use of the paternally inherited *Sox2-Cre* transgene, recombining the *Ecto* conditional allele in the epiblast lineage specifically (*Sox2-Cre; Ecto fl/-* embryos, hereafter *Ecto-EpiKO*; see Fig. S1G,H in the supplementary material for epiblast-specific protein depletion) (Hayashi et al., 2002; Di-Gregorio et al., 2007). In *EpiKO* mutants, a genetically wild-type AVE did not display any of the abnormalities characterizing the *Ecto* germline mutants, as *Cerl* and *Lefty1* mRNAs were comparable in localization and intensity with wild-type embryos (Fig. 1M,N and not shown). In line with a cell-autonomous role for Ecto in AVE cells, at E5.5, *Nodal* is expressed normally in *Ecto* mutant embryos (Fig. 1O,P) and, by immunofluorescence, Smad2 phosphorylation is comparable between wild type and *Ecto* mutants (Fig. 1Q,R). This is in agreement with our previous observations indicating that Ecto inhibits TGFβ signaling acting specifically on Smad4 availability and not on R-Smads (Dupont et al., 2009). Together, these findings suggest that *Ecto* is required cell-autonomously to restrain Nodal responsiveness in AVE cells.

Defective AVE patterning of *Ecto* mutants is caused by unrestrained Nodal/Smad4 signaling

The phenotype of *Ecto*$^{-/-}$ embryos is opposite to those reported for *Nodal*, *Smad2* and *Smad4* knockouts (Brennan et al., 2001; Waldrip et al., 1998; Yang et al., 1998). Hence, we investigated the genetic relationships between *Ecto* and its biochemical target *Smad4* (Dupont et al., 2009). We analyzed embryos from crosses of mice carrying the floxed alleles for the two genes (*Ecto fl/–* and *Smad4 fl/–*) that were undergoing zygotic deletion in the *CAG-Cre* maternal background (Sakai and Miyazaki, 1997) (see Materials and methods for details). *Ecto fl/–;CAG-Cre* embryos lacked of endogenous Ecto protein (not shown) and were phenotypically indistinguishable from *Ecto* germline homozygous mutants (compare Fig. 2B,F with Fig. 1F,H); *Smad4 fl/–;CAG-Cre* phenocopied morphologically the previously reported defects of the null allele (Yang et al., 1998). Extending these studies, we found that *Smad4* is dispensable for VE specification (as revealed by the detection of the *Afp* marker, see Fig. S3 in the supplementary material), but required for *Cerl* and *Lim1* induction (Fig. 2C,G). In line with previous biochemical findings, double mutants for *Smad4* and *Ecto* were indistinguishable from *Smad4* mutants (Fig. 2C,D,G,H). Thus, *Ecto* acts as inhibitor of *Smad4*-dependent signaling, and does not regulate AVE formation through an alternative *Smad4*-independent pathway.

Data presented so far suggest that disruption of the Ecto/Smad4 inhibitory axis leads to excessive Nodal responsiveness in AVE. If so, this should be rebalanced by a concomitant reduction of the Nodal dose. To this end, we combined *Ecto* mutant with a strongly attenuated *Nodal* mutant (*NodalΔ600/–*) (Norris et al., 2002), leading to a rescue of AVE patterning (Fig. 2I-K). Taking into account the cell-autonomous role of *Ecto* shown above, these results collectively suggest that the net activity of Nodal signaling, at least for AVE induction, is the result of two components: extracellular ligand availability and negative control of Smad responsiveness. Loss of the latter in *Ecto* mutants is sufficient to profoundly alter embryonic patterning.

Ecto maintains EXE self-renewal by opposing *Nodal* signaling

Next, we characterized molecularly the development in *Ecto* mutants of the other extra-embryonic tissue, the trophoblast lineage. As shown in Fig. 3, the trophoblast stem (TS) cells and EXE markers *Eomes*, *Cdx2* and *Bmp4* were undetectable in E5.5

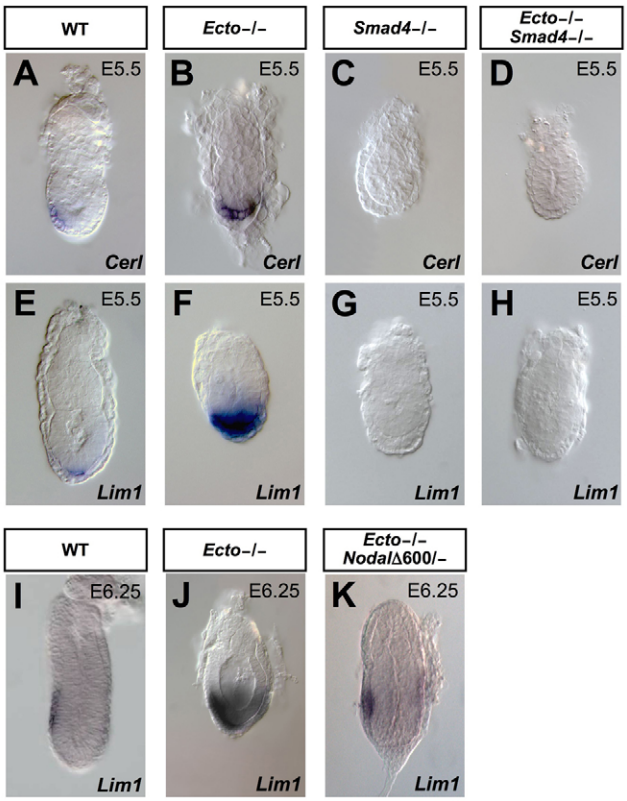

Fig. 2. Defective AVE patterning in *Ecto* mutants is mediated by *Smad4* and is due to unrestrained Nodal signaling. (**A-H**) Excessive AVE formation in *Ecto* mutants is dependent on Smad4 activity. In situ hybridization for the AVE markers *Cerl* and *Lim1* in wild-type (A,E), *Ecto*$^{-/-}$ (B,F), *Smad4*$^{-/-}$ (C,G) and *Ecto/Smad4* double mutant embryos (D,H). AVE expansion is observed in *Ecto* mutants but not in embryos also lacking *Smad4* (D,H). In *Smad4*-deficient embryos AVE is not induced (C,G) but VE is correctly specified (see *AFP* staining in Fig. S3, in the supplementary material). (**I-K**) Reduction of Nodal signaling by the combined use of null (*Nodal–*) and hypomorphic (*NodalΔ600*) alleles counterbalances AVE expansion in *Ecto* mutants, as assayed by in situ hybridization for *Lim1* at pre-streak stage (compare J with K). In K, decreased *Nodal* also rescues the overall morphology and size of the *Ecto* mutants. Compare J with Fig. 5J for an example of phenotypic variation. Lateral views, anterior towards the left.

Ecto$^{-/-}$ embryos (Fig. 3A-F). This represents a cell-autonomous requirement as *Ecto-EpiKO* embryos displayed normal EXE development (Fig. 3G,H). Lack of EXE in *Ecto* mutants is paradoxically similar to the phenotype of *Nodal* mutants (Brennan et al., 2001); however, in the case of *Nodal*, this is secondary to defective epiblast patterning where *Nodal* sustains *Oct4* and *Fgf4* transcription, which, in turn, maintains TS self-renewal (Guzman-Ayala et al., 2004; Lu and Robertson, 2004; Mesnard et al., 2006). By contrast, *Fgf4* and *Oct4* are normally expressed in *Ecto* mutants (Fig. 3I-L). Strikingly, Nodal attenuation rescued the EXE phenotype of *Ecto* mutants, as *Eomes* and *Bmp4* transcripts were invariably rescued in combined *Ecto*$^{-/-}$*; NodalΔ600/–* or *Ecto*$^{-/-}$*; Nodal*$^{+/-}$ embryos (Fig. 3M-P for *Bmp4* expression, see Fig. 5A-D for *Eomes*). Taken together, these data suggest that *Ecto* protects the TS lineage from excessive Nodal signaling.

To understand the nature of *Ecto* function in EXE, we monitored TS induction from earlier developmental stages. At earlier stages, *Cdx2* was expressed in *Ecto* mutants (Fig. 4A,B), indicating that

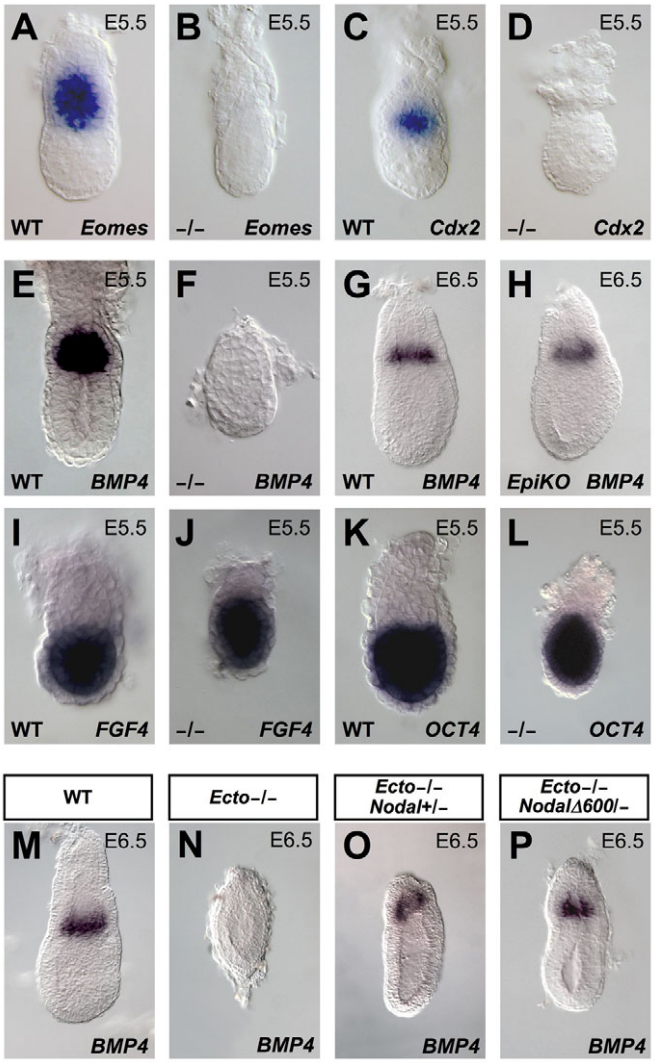

Fig. 3. *Ecto* maintains EXE self-renewal by opposing Nodal signaling. (**A-F**) *Ecto* mutants lack expression of trophoblast stem (TS) cell markers *Eomes* (A,B), *Cdx2* (C,D) and *Bmp4* (E,F) at E5.5. (**G**,**H**) *Ecto* acts cell-autonomously within the extra-embryonic tissues to maintain EXE fates. Panels show in situ for *Bmp4* in wild-type and *Sox2-Cre;Ecto fl/–* (*Ecto-EpiKO*) embryos, i.e. in embryos where *Ecto* is inactivated in epiblast cells, but not in extra-embryonic tissues. (**I-L**) The epiblast markers *Fgf4* (I,J) and *Oct4* (K,L) are normally expressed in *Ecto* mutants. (**M-P**) Reduction of *Nodal* dose rescues EXE formation in *Ecto* mutant embryos, as assayed by *Bmp4* expression.

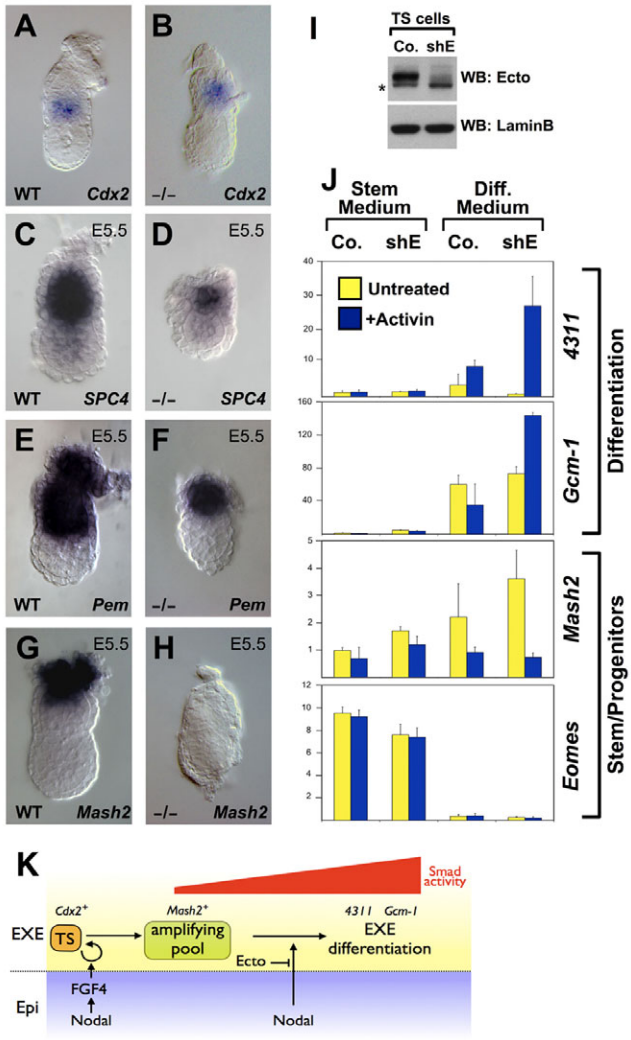

Fig. 4. *Ecto* prevents Nodal/TGFβ-induced differentiation of trophoblast stem (TS) cells. (**A**,**B**) The trophoblast lineage is correctly specified in *Ecto* mutants, as assayed by *Cdx2* expression at early post-implantation stages. (**C-F**) *Ecto* mutants retain *Spc4* (C,D) and *Pem* (E,F) expression within the differentiated trophoplast/ectoplacental cone. (**G**,**H**) The trophoblast early differentiation/transient-amplifying marker *Mash2* is lacking in *Ecto* mutants. (**I**) Immunoblotting for Ecto shows efficient protein depletion in TS cells stably expressing Ecto shRNA (shE). LaminB serves as loading control. Asterisk indicates a non-specific band detected by the anti-Ecto antibody. (**J**) Real-time qPCR analysis of TS cell markers. Control (Co.) and Ecto shRNA-depleted (shE) TS cells were cultivated in self-renewing conditions (Stem Medium) or induced to differentiate for 4 days (Diff. Medium), in the absence or presence of activin protein in the culture medium, mimicking Nodal stimulation. *4311* and *Gcm1* are trophoblast differentiation markers, *Mash2* is a transient-amplifying marker and *Eomes* is a stem-cell marker. Values are given relative to *Gapdh* expression. Note how TS cells undergo precocious differentiation only in the absence of Ecto and in the presence of TGFβ stimulation (+Activin). Data from a representative experiment are presented as mean±s.d. of two replicates. See also Fig. S4 in the supplementary material for a quantitation of mitotic cells in wild-type and *Ecto* mutant embryos. (**K**) Model of the role and control of Nodal signaling in the homeostasis of EXE.

excessive Nodal responsiveness affects later events. We then monitored cell viability, and found comparable apoptosis and proliferation rates in wild-type and mutant embryos (see Fig. S4 in the supplementary material; and data not shown). As development proceeds, we found that *Ecto* mutants do retain expression of *Spc4* (*Pcsk6* – Mouse Genome Informatics) and *Pem* (*Rhox5* – Mouse Genome Informatics) identifying the presence of more differentiated cells of the ectoplacental cone (Constam and Robertson, 2000; Lin et al., 1994) (Fig. 4C-F), but lose expression of *Mash2* (*Ascl2* – Mouse Genome Informatics), a marker for transit-amplifying trophoblast progenitors (Guillemot et al., 1995) (Fig. 4G,H). These data suggest that Nodal signaling also plays a direct role on trophoblast cells, promoting their differentiation.

To validate this hypothesis, we established control (shGFP) and Ecto-depleted (shEcto) mouse TS populations by lentiviral infection, and compared them for the expression of stem and differentiation

markers (Fig. 4I,J). When cultured in stemness/proliferating medium, Control and shEcto TS cells were comparable in terms of marker expressions and cell cycle profiles (Fig. 4J and not shown), reinforcing the notion that *Ecto* is not required for TS cells induction or self-renewal. However, once TS cells were induced to differentiate, in the presence of the Nodal-related ligand Activin shEcto cells specifically displayed a robust increase in the expression of differentiation markers *4311* (Tanaka et al., 1998) and *Gcm1* (Anson-Cartwright et al., 2000) (Fig. 4J), recapitulating in vitro our observations on *Ecto* mutants. Comparable results were obtained with an independent shRNA targeting Ecto (not shown). Tight control over Nodal activity is thus crucial for balancing stem cells renewal and differentiation in the trophoblast lineage; in *Ecto* mutants, uncontrolled Nodal signaling causes wholesale exhaustion of the stem cell pool (see model in Fig. 4K).

Nodal attenuation rescues mesoderm formation in *Ecto* mutants

By losing the EXE, *Ecto* mutants are deprived of an essential source of mesoderm inducing and patterning signals, including BMP4 (Arnold and Robertson, 2009); at the same time, they display enhanced expression of Nodal antagonists, such as Cerl and Lefty1. This raises questions about the primary cause of defective mesoderm in *Ecto* mutants. Remarkably, attenuation of Nodal signaling in compound *Ecto/Nodal* mutants rescues mesoderm development, as revealed by transcription of the pan-mesodermal markers *Eomes* and *T* at the early gastrula stage (Fig. 5A-H). Interestingly, although the combination $Ecto^{-/-}$; *NodalΔ600/–* rescues EXE, mesoderm and AVE (Fig. 5D,H and Fig. 2K), compound $Ecto^{-/-}$; $Nodal^{+/-}$ could rescue defective EXE and mesoderm but not AVE expansion (compare Fig. 5C,G with Fig. 5K). This suggests that lack of mesoderm in *Ecto* mutants is primarily due to lack of EXE; molecularly, this can be explained by the failure to induce BMP4 expression (Fig. 3) that represents an important mediator of a feed-forward loop between the EXE and epiblast feeding on *Nodal* expression and mesoderm induction (Arnold and Robertson, 2009).

A further complicating issue is the fact that AVE and EXE development might be linked, as the EXE has also been proposed to secrete AVE inhibiting factors (Rodriguez et al., 2005; Yamamoto et al., 2009). Is then the AVE expansion observed in *Ecto* mutants due to loss of EXE? Our results suggest this is not the case, because in $Ecto^{-/-}$; $Nodal^{+/-}$ embryos these events are uncoupled (compare Fig. 3O and Fig. 5K): these compound mutants display rescued EXE in the presence of a still expanded AVE. Thus, data support the view that expanded AVE in *Ecto* mutants is primarily due to enhanced Nodal responsiveness of the visceral endoderm. Clearly, the loss of BMP expression in the EXE might amplify, to some extent, the enlarged AVE domain of the Ecto mutants.

A role for *Ecto* in restraining anterior meso-endoderm formation

The *Sox2-Cre; Ecto fl/–* embryos (*Ecto-EpiKO*) allow the more direct study of the role of *Ecto* in the epiblast, bypassing its early requirements in extra-embryonic tissues. Previous work established that a gradient of Nodal/Smad *activity* patterns the primitive streak (Dunn et al., 2004; Lowe et al., 2001; Vincent et al., 2003); in this context, *Smad4* is required for peak signaling levels, namely, for the formation of the anterior primitive streak and node, marked by *Foxa2* expression (Chu et al., 2004). Strikingly, we found that approximately one-third (4/13) of the *Ecto-EpiKO* embryos displayed an expanded *Foxa2* expression at streak stages (Fig. 6A-6B′). These embryos appeared smaller, lacked an overtly elongated streak and probably failed to undergo proper gastrulation. At later stages, surviving *Ecto-EpiKO* embryos showed expansion of the Node (marked by *Foxa2* staining, Fig. 6C,D), an almost radial expansion of the definitive endoderm marker *Cerl* (Fig. 6E,F), as well as duplications of Node and anterior axial mesendoderm tissues (*T*, *Shh* and *Chordin* in situs, Fig. 6G-J and not shown). Together, the data suggest that *Ecto* is essential for orchestrating the intensity of Nodal/Smad4 responses for proper primitive streak development. These early defects of *Ecto-EpiKO* are such that loss of *Ecto* in epiblast cells is incompatible with subsequent development. Indeed, we could identify only few *Ecto-EpiKO* embryos at E10.0, displaying defective brain development and open neural folds (not shown).

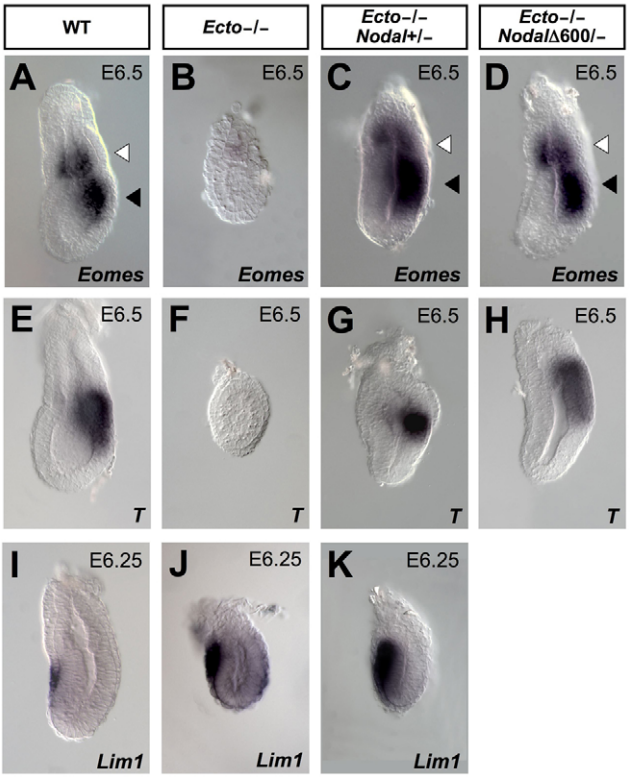

Fig. 5. Lack of mesoderm in *Ecto* mutants is caused by excessive *Nodal* and linked to defective EXE development. (**A-H**) Reduction of *Nodal* rescues mesoderm formation in *Ecto* mutant embryos, as assayed by *Eomes* expression (A-D, black arrowheads) and *T* (E-H). Lateral views, anterior towards the left. (**I-K**) Analysis of *Lim1* expression in AVE of wild-type, *Ecto* mutants and $Ecto^{-/-}$; $Nodal^{+/-}$ embryos. $Ecto^{-/-}$; $Nodal^{+/-}$ embryos show already rescued mesoderm (C,G) and EXE development (white arrowheads), but still display expanded AVE (K).

DISCUSSION

In this paper, we show that cell-autonomous Smad regulation operated by the Smad4 ubiquitin-ligase ectodermin is essential to dose Nodal responsiveness in mouse embryos. Analysis of *Ecto* mutants showed that loss of *Ecto* 'upgrades' Nodal responses in extra-embryonic and embryonic lineages.

In the visceral endoderm, unrestrained Nodal responsiveness causes a massive expansion of the *Cerl/Lefty1* expressing AVE territory; this is *Smad4*-dependent and can be rescued by

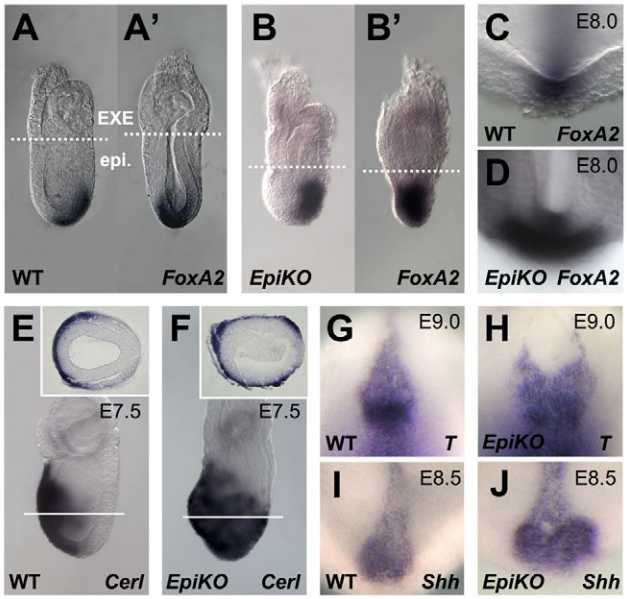

Fig. 6. Expansion of the organizer in epiblast-specific *Ecto* mutants. (**A-B'**) Expression of the anterior mesoderm marker *Foxa2* encompasses the whole primitive streak in *Sox2-Cre;Ecto fl/–* (*Ecto-EpiKO*) streak stage embryos. (A,A′) Lateral and posterior views of a wild-type embryo. (B,B′) Lateral and posterior views of an *Ecto-EpiKO* embryo. Broken lines indicate the boundary between extra-embryonic (EXE) and embryonic (epi.) tissues. (**C**,**D**) Expansion of the node in *Ecto-EpiKO* embryos. Pictures show a higher magnification of the distal region of sibling embryos stained for the node marker *Foxa2*, taken from the anterior. (**E**,**F**) In situ hybridization for the definitive endoderm marker *Cerl* at E7.5. Lateral views, anterior towards the left. Insets show transverse sections of the corresponding embryos, taken at the level of white lines. (**G-J**) *Ecto-EpiKO* embryos display a widened and duplicated anterior node, as assayed by expression of *T* (G,H) and *Shh* (I,J) at E8.5/9.0. Images show a higher magnification of the node region, anterior towards the top. See Fig. S5 in the supplementary material for whole embryo lateral views used for staging purposes.

reducing the dosage of *Nodal*. Thus, it appears that, in vivo, the net activity of Nodal/TGFβ is the result of a combination of two elements: extracellular ligand availability, which is defined by the expression of Nodal and its antagonists, and translates into receptor activation and Smad2/3 phosphorylation; and negative control over Smad4 availability. In *Ecto* mutants, loss of this second layer of control is sufficient to profoundly alter embryonic patterning.

Novel functions of Nodal are revealed by this analysis. In the EXE, excess of Nodal responsiveness in *Ecto* mutants leads to the wholesale differentiation and exhaustion of the trophoblast stem (TS) cell compartment. This had not previously inferred by Nodal or Smad loss-of-function analyses. Indeed, in *Nodal* mutants, EXE is induced but not maintained, a phenotype that superficially overlaps with that of *Ecto* mutants. Marker analysis in fact revealed a profound difference: although in *Nodal* mutants the trophoblast transient amplifying progenitors become expanded (Guzman-Ayala et al., 2004), in *Ecto* mutants this cellular pool is instead depleted, in favor of more differentiated cellular progenies (Fig. 4). This suggests that Nodal signaling drives – and Ecto inhibits – trophoblast differentiation; the ensuing equilibrium allows the homeostatic expansion and differentiation of trophoblast progenitors.

Secondary to deficiencies in extra-embryonic tissues, *Ecto* mutants ultimately lack primitive streak and mesoderm induction; notably, this defect in the embryo proper can be paradoxically rescued by a reduction of *Nodal* dose, because this normalizes extra-embryonic development. Mesoderm induction requires inputs from the EXE but is inhibited by Nodal antagonists emanating from the AVE; these are respectively missing and enhanced in *Ecto* mutants. So, what is the nature of their mesodermal defect? Our data suggest a primary role in the defective EXE, as in combined $Ecto^{-/-}$; $Nodal^{+/-}$ embryos the AVE remains expanded but EXE and mesoderm formation is rescued.

In the epiblast, the generation of different mesoderm and endoderm derivatives appears to be a response to exposure to different intensities of Nodal signaling (Dunn et al., 2004; Lowe et al., 2001; Vincent et al., 2003). Although complete loss of Nodal prevents germ layer formation, smaller reductions primarily affect the anterior derivatives of the primitive streak. Similarly, *Smad4* appears required for anterior but not posterior primitive streak derivatives (Chu et al., 2004). However, it remains unclear whether an anteroposterior extracellular Nodal gradient exists, also considering that Nodal is evenly expressed along the primitive streak (Tam and Loebel, 2007). Our data suggest that intracellular control of Smad activity by Ecto plays a crucial role in these morphogenetic effects. In contrast to *Smad4* deficiencies, loss of Ecto leads to an expansion of anterior primitive streak and its derivatives, including Node and definitive endoderm.

This work also contributes towards resolving an issue regarding the function of ectodermin/Tif1γ in TGFβ signal transduction. We have discovered Ecto as TGFβ antagonist in an unbiased expression screen for determinants of germ-layer identity in the frog embryo (Dupont et al., 2005); others independently isolated the same molecule biochemically, as a Smad-interacting factor, and suggested that Ecto may act as Smad2/3 partner to mediate an alternative Smad4-independent TGFβ pathway (He et al., 2006). However, our genetic evidence supports the view of Ecto as inhibitor of canonical Nodal/TGFβ signaling, as defects of *Ecto* mutants depend on *Smad4* and are rescued by reducing *Nodal* dose.

In summary, this study reveals how cell-autonomous negative modulation of Smads signaling endows embryonic cells with distinct interpretational keys to Nodal signals. This orchestrates the development of embryonic cells into distinct pluripotent cell lineages of the early mouse embryo and, probably, adult tissue homeostasis. An interesting possibility for future studies will be to determine whether Ecto activities are themselves patterned in vivo and whether this crucial regulatory layer can be exploited therapeutically in diseases characterized by excess of TGFβ activity, such as fibrosis or metastasis.

Acknowledgements
This paper is dedicated to Regine Losson who recently passed away. We thank J. Collignon, T. Rodriguez, J. Rossant, J. A. Belo, D. Constam, M. Pfeffer, S. Thilgam, G. Liguori for gifts of plasmids and cell lines. We are particularly grateful to E. J. Robertson for providing us *Nodal-lacZ*, *NodalΔ600* and *Sox2-Cre* mice, to R. DePinho for *Smad4-floxed* mice and to J. Miyazaki for the *CAG-Cre* line. M. Cordenonsi, O. Wessely, G. Minchiotti, D. Volpin and all members of the Piccolo group offered invaluable discussions and comments on the manuscript. This work is supported by grants from the Centre National de la Recherche Scientifique (CNRS) to R.L. and from Fondazione Telethon, Italian Association on Cancer Research (AIRC) and Fondazione Cariparo (Excellence-grant) to S.P. and S.D. E.E. is recipient of a Fondazione Cariparo PhD fellowship.

Competing interests statement
The authors declare no competing financial interests.

Author contributions

L.M., S.D. and S.P. designed experiments and analyzed data. L.M. performed in situs and post in situ embryo genotyping; E.E. performed breedings, immunofluorescence staining and helped with in situs; M.A. performed real-time PCR and TS cell experiments with S.D., and colony genotyping with S.S.; K.Y., O.W., M.M., K.K., P.C. and R.L. designed and generated the *Ecto* knockout alleles; S.P. and S.D. wrote the paper.

Supplementary material

Supplementary material for this article is available at
http://dev.biologists.org/lookup/suppl/doi:10.1242/dev.053801/-/DC1

References

Adorno, M., Cordenonsi, M., Montagner, M., Dupont, S., Wong, C., Hann, B., Solari, A., Bobisse, S., Rondina, M. B., Guzzardo, V. et al. (2009). A Mutant-p53/Smad complex opposes p63 to empower TGFbeta-induced metastasis. *Cell* **137**, 87-98.

Anson-Cartwright, L., Dawson, K., Holmyard, D., Fisher, S. J., Lazzarini, R. A. and Cross, J. C. (2000). The glial cells missing-1 protein is essential for branching morphogenesis in the chorioallantoic placenta. *Nat. Genet.* **25**, 311-314.

Arnold, S. J. and Robertson, E. J. (2009). Making a commitment: cell lineage allocation and axis patterning in the early mouse embryo. *Nat. Rev. Mol. Cell Biol.* **10**, 91-103.

Bachiller, D., Klingensmith, J., Kemp, C., Belo, J. A., Anderson, R. M., May, S. R., McMahon, J. A., McMahon, A. P., Harland, R. M., Rossant, J. et al. (2000). The organizer factors Chordin and Noggin are required for mouse forebrain development. *Nature* **403**, 658-661.

Bardeesy, N., Cheng, K. H., Berger, J. H., Chu, G. C., Pahler, J., Olson, P., Hezel, A. F., Horner, J., Lauwers, G. Y., Hanahan, D. et al. (2006). Smad4 is dispensable for normal pancreas development yet critical in progression and tumor biology of pancreas cancer. *Genes Dev.* **20**, 3130-3146.

Brennan, J., Lu, C. C., Norris, D. P., Rodriguez, T. A., Beddington, R. S. and Robertson, E. J. (2001). Nodal signalling in the epiblast patterns the early mouse embryo. *Nature* **411**, 965-969.

Cammas, F., Mark, M., Dolle, P., Dierich, A., Chambon, P. and Losson, R. (2000). Mice lacking the transcriptional corepressor TIF1beta are defective in early postimplantation development. *Development* **127**, 2955-2963.

Chu, G. C., Dunn, N. R., Anderson, D. C., Oxburgh, L. and Robertson, E. J. (2004). Differential requirements for Smad4 in TGFbeta-dependent patterning of the early mouse embryo. *Development* **131**, 3501-3512.

Collignon, J., Varlet, I. and Robertson, E. J. (1996). Relationship between asymmetric nodal expression and the direction of embryonic turning. *Nature* **381**, 155-158.

Constam, D. B. and Robertson, E. J. (2000). SPC4/PACE4 regulates a TGFbeta signaling network during axis formation. *Genes Dev.* **14**, 1146-1155.

Di-Gregorio, A., Sancho, M., Stuckey, D. W., Crompton, L. A., Godwin, J., Mishina, Y. and Rodriguez, T. A. (2007). BMP signalling inhibits premature neural differentiation in the mouse embryo. *Development* **134**, 3359-3369.

Dunn, N. R., Vincent, S. D., Oxburgh, L., Robertson, E. J. and Bikoff, E. K. (2004). Combinatorial activities of Smad2 and Smad3 regulate mesoderm formation and patterning in the mouse embryo. *Development* **131**, 1717-1728.

Dupe, V., Davenne, M., Brocard, J., Dolle, P., Mark, M., Dierich, A., Chambon, P. and Rijli, F. M. (1997). In vivo functional analysis of the Hoxa-1 3′ retinoic acid response element (3′RARE). *Development* **124**, 399-410.

Dupont, S., Zacchigna, L., Cordenonsi, M., Soligo, S., Adorno, M., Rugge, M. and Piccolo, S. (2005). Germ-layer specification and control of cell growth by Ectodermin, a Smad4 ubiquitin ligase. *Cell* **121**, 87-99.

Dupont, S., Mamidi, A., Cordenonsi, M., Montagner, M., Zacchigna, L., Adorno, M., Martello, G., Stinchfield, M. J., Soligo, S., Morsut, L. et al. (2009). FAM/USP9x, a deubiquitinating enzyme essential for TGFbeta signaling, controls Smad4 monoubiquitination. *Cell* **136**, 123-135.

Guillemot, F., Caspary, T., Tilghman, S. M., Copeland, N. G., Gilbert, D. J., Jenkins, N. A., Anderson, D. J., Joyner, A. L., Rossant, J. and Nagy, A. (1995). Genomic imprinting of Mash2, a mouse gene required for trophoblast development. *Nat. Genet.* **9**, 235-242.

Guzman-Ayala, M., Ben-Haim, N., Beck, S. and Constam, D. B. (2004). Nodal protein processing and fibroblast growth factor 4 synergize to maintain a trophoblast stem cell microenvironment. *Proc. Natl. Acad. Sci. USA* **101**, 15656-15660.

Hayashi, S., Lewis, P., Pevny, L. and McMahon, A. P. (2002). Efficient gene modulation in mouse epiblast using a Sox2Cre transgenic mouse strain. *Mech. Dev.* **119**, S97-S101.

He, W., Dorn, D. C., Erdjument-Bromage, H., Tempst, P., Moore, M. A. and Massague, J. (2006). Hematopoiesis controlled by distinct TIF1gamma and Smad4 branches of the TGFbeta pathway. *Cell* **125**, 929-941.

Itoh, S. and ten Dijke, P. (2007). Negative regulation of TGF-beta receptor/Smad signal transduction. *Curr. Opin. Cell Biol.* **19**, 176-184.

Lin, T. P., Labosky, P. A., Grabel, L. B., Kozak, C. A., Pitman, J. L., Kleeman, J. and MacLeod, C. L. (1994). The Pem homeobox gene is X-linked and exclusively expressed in extraembryonic tissues during early murine development. *Dev. Biol.* **166**, 170-179.

Lin, X., Duan, X., Liang, Y. Y., Su, Y., Wrighton, K. H., Long, J., Hu, M., Davis, C. M., Wang, J., Brunicardi, F. C. et al. (2006). PPM1A functions as a Smad phosphatase to terminate TGFbeta signaling. *Cell* **125**, 915-928.

Lowe, L. A., Yamada, S. and Kuehn, M. R. (2001). Genetic dissection of nodal function in patterning the mouse embryo. *Development* **128**, 1831-1843.

Lu, C. C. and Robertson, E. J. (2004). Multiple roles for Nodal in the epiblast of the mouse embryo in the establishment of anterior-posterior patterning. *Dev. Biol.* **273**, 149-159.

Mesnard, D., Guzman-Ayala, M. and Constam, D. B. (2006). Nodal specifies embryonic visceral endoderm and sustains pluripotent cells in the epiblast before overt axial patterning. *Development* **133**, 2497-2505.

Moffat, J., Grueneberg, D. A., Yang, X., Kim, S. Y., Kloepfer, A. M., Hinkle, G., Piqani, B., Eisenhaure, T. M., Luo, B., Grenier, J. K. et al. (2006). A lentiviral RNAi library for human and mouse genes applied to an arrayed viral high-content screen. *Cell* **124**, 1283-1298.

Moustakas, A. and Heldin, C. H. (2009). The regulation of TGFbeta signal transduction. *Development* **136**, 3699-3714.

Norris, D. P., Brennan, J., Bikoff, E. K. and Robertson, E. J. (2002). The Foxh1-dependent autoregulatory enhancer controls the level of Nodal signals in the mouse embryo. *Development* **129**, 3455-3468.

Oda, M., Shiota, K. and Tanaka, S. (2006). Trophoblast stem cells. *Methods Enzymol.* **419**, 387-400.

Perea-Gomez, A., Vella, F. D., Shawlot, W., Oulad-Abdelghani, M., Chazaud, C., Meno, C., Pfister, V., Chen, L., Robertson, E., Hamada, H. et al. (2002). Nodal antagonists in the anterior visceral endoderm prevent the formation of multiple primitive streaks. *Dev. Cell* **3**, 745-756.

Rodriguez, T. A., Srinivas, S., Clements, M. P., Smith, J. C. and Beddington, R. S. (2005). Induction and migration of the anterior visceral endoderm is regulated by the extra-embryonic ectoderm. *Development* **132**, 2513-2520.

Sakai, K. and Miyazaki, J. (1997). A transgenic mouse line that retains Cre recombinase activity in mature oocytes irrespective of the cre transgene transmission. *Biochem. Biophys. Res. Commun.* **237**, 318-324.

Tam, P. P. and Loebel, D. A. (2007). Gene function in mouse embryogenesis: get set for gastrulation. *Nat. Rev. Genet.* **8**, 368-381.

Tanaka, S., Kunath, T., Hadjantonakis, A. K., Nagy, A. and Rossant, J. (1998). Promotion of trophoblast stem cell proliferation by FGF4. *Science* **282**, 2072-2075.

Vincent, S. D., Dunn, N. R., Hayashi, S., Norris, D. P. and Robertson, E. J. (2003). Cell fate decisions within the mouse organizer are governed by graded Nodal signals. *Genes Dev.* **17**, 1646-1662.

Waldrip, W. R., Bikoff, E. K., Hoodless, P. A., Wrana, J. L. and Robertson, E. J. (1998). Smad2 signaling in extraembryonic tissues determines anterior-posterior polarity of the early mouse embryo. *Cell* **92**, 797-808.

Yamamoto, M., Beppu, H., Takaoka, K., Meno, C., Li, E., Miyazono, K. and Hamada, H. (2009). Antagonism between Smad1 and Smad2 signaling determines the site of distal visceral endoderm formation in the mouse embryo. *J. Cell Biol.* **184**, 323-334.

Yan, K. P., Dolle, P., Mark, M., Lerouge, T., Wendling, O., Chambon, P. and Losson, R. (2004). Molecular cloning, genomic structure, and expression analysis of the mouse transcriptional intermediary factor 1 gamma gene. *Gene* **334**, 3-13.

Yang, X., Li, C., Xu, X. and Deng, C. (1998). The tumor suppressor SMAD4/DPC4 is essential for epiblast proliferation and mesoderm induction in mice. *Proc. Natl. Acad. Sci. USA* **95**, 3667-3672.

Zacchigna, L., Vecchione, C., Notte, A., Cordenonsi, M., Dupont, S., Maretto, S., Cifelli, G., Ferrari, A., Maffei, A., Fabbro, C. et al. (2006). Emilin1 links TGF-beta maturation to blood pressure homeostasis. *Cell* **124**, 929-942.